

THE INFLUENCE OF HILLY TERRAIN ON CANOPY-ATMOSPHERE CARBON DIOXIDE EXCHANGE

G. G. KATUL^{1,*}, J. J. FINNIGAN², D. POGGI^{1,3}, R. LEUNING² and
S. E. BELCHER⁴

¹*Nicholas School of the Environment and Earth Sciences, Box 90328, Duke University, Durham, NC 27708-0328, U.S.A.*; ²*CSIRO Atmospheric Research, FC Pye Laboratory, Black Mountain, Canberra, ACT 2601, Australia*; ³*Dipartimento di Idraulica, Trasporti ed Infrastrutture Civili Politecnico di Torino, Torino, Italy*; ⁴*Department of Meteorology, University of Reading, Reading, RG6 6BB, U.K.*

(Received in final form 20 April 2005)

Abstract. Topography influences many aspects of forest-atmosphere carbon exchange; yet only a small number of studies have considered the role of topography on the structure of turbulence within and above vegetation and its effect on canopy photosynthesis and the measurement of net ecosystem exchange of CO₂ (N_{ec}) using flux towers. Here, we focus on the interplay between radiative transfer, flow dynamics for neutral stratification, and ecophysiological controls on CO₂ sources and sinks within a canopy on a gentle cosine hill. We examine how topography alters the forest-atmosphere CO₂ exchange rate when compared to uniform flat terrain using a newly developed first-order closure model that explicitly accounts for the flow dynamics, radiative transfer, and nonlinear ecophysiological processes within a plant canopy. We show that variation in radiation and airflow due to topography causes only a minor departure in horizontally averaged and vertically integrated photosynthesis from their flat terrain values. However, topography perturbs the airflow and concentration fields in and above plant canopies, leading to significant horizontal and vertical advection of CO₂. Advection terms in the conservation equation may be neglected in flow over homogeneous, flat terrain, and then $N_{ec} = F_c$, the vertical turbulent flux of CO₂. Model results suggest that vertical and horizontal advection terms are generally of opposite sign and of the same order as the biological sources and sinks. We show that, close to the hilltop, F_c departs by a factor of three compared to its flat terrain counterpart and that the horizontally averaged F_c -at canopy top differs by more than 20% compared to the flat-terrain case.

Keywords: Advection, Biosphere-atmosphere exchange, Canopy flow, Complex terrain, Gentle hills, Net ecosystem exchange, Photosynthesis.

1. Introduction

Topography influences almost all aspects of forest-atmosphere carbon exchange and storage through spatial variation in vegetation type, soil

* E-mail: gaby@duke.edu

texture, depth and hydraulic properties, nutrient availability and respiring biomass. Topography also affects canopy microclimate through radiative transfer, thermodynamic processes, and flow dynamics (see Raupach and Finnigan, 1997 for a review). Because of the numerous interactions and non-linear feedback amongst all these processes, the manner in which topography alters forest-atmosphere carbon exchange is a vexing question. To begin to address this problem, we must limit our attention to the most basic processes that control photosynthesis (A_n) and net carbon dioxide fluxes (F_c), namely the interplay between radiative forcing, flow dynamics, and ecophysiological controls on CO_2 sources and sinks within the canopy. To progress even within this restricted compass, many of the governing processes must be simplified and parameterized.

The work we describe extends previous work on quantifying scalar transport on gentle hilly terrain (Raupach et al., 1992; Raupach and Finnigan, 1997) by resolving the flow dynamics, radiative transfer, and non-linear ecophysiological processes within and above a canopy on a hill. The interplay between these three processes for canopies in hilly terrain is the main novelty of the present work.

We use the new theory to examine the errors that occur in determining photosynthesis and CO_2 fluxes when assumptions appropriate to flat terrain are applied to measurements over forests on hills. In particular, we quantify the relative importance of advective and turbulent flux divergence terms in the mass balance equation that underpins surface exchange measurements from towers in complex terrain. This comparison is of particular significance to the rapidly growing number of eddy covariance flux monitoring sites around the globe (Balocchi et al., 2001), many of which are situated in complex topography.

2. Theory

The model of scalar flow and transport that we will use is based on the analytic wind-field model of Finnigan and Belcher (2004), (henceforth FB04). This is a first-order two-dimensional closure model of turbulent flow over and within a tall canopy on a low or gentle hill and serves as a logical starting point for such an investigation.

We consider well-watered uniform vegetation, of height h_c , on a cosine-shaped hill beneath a non-stratified atmospheric flow (Figure 1). The presence of the hill creates a pressure perturbation that to first order in the hill slope is vertically uniform through the shear stress layer (defined below) and the canopy (FB04). This pressure perturbation drives horizontal and vertical gradients in mean velocity across the hill and these gradients in turn introduce advective terms and spatial variability in

divide the airflow over the hill into a thin inner *shear stress* layer of depth l_i , and an outer layer. Below l_i mean flow perturbations caused by the hill are affected to first order in H/L by perturbations in shear stress. Conversely, in the outer layer the dynamics of flow perturbations are essentially inviscid. Recent reviews of key numerical, experimental, and analytical approaches can be found in Taylor et al. (1987), Finnigan (1988), Hunt et al. (1988), Carruthers and Hunt (1990), Kaimal and Finnigan (1994), Raupach and Finnigan (1997), Belcher and Hunt (1998), Wilson et al. (1998), Finnigan and Belcher (2004), and Finnigan (2004). The novelty of the present work is that the canopy sublayer is treated as a ‘dynamically distinct’ atmospheric layer interacting with the inner and outer layers.

Within the canopy layer, the two-dimensional mean continuity and momentum balance for stationary, high Reynolds number and neutrally stratified turbulent flows are given by FB04,

$$\frac{\partial \bar{u}}{\partial x} + \frac{\partial \bar{w}}{\partial z} = 0, \quad (1)$$

$$\bar{u} \frac{\partial \bar{u}}{\partial x} + \bar{w} \frac{\partial \bar{u}}{\partial z} = -\frac{1}{\rho} \frac{\partial \bar{p}}{\partial x} - \left(\frac{\partial \overline{u'u'}}{\partial x} + \frac{\partial \overline{u'w'}}{\partial z} \right) - F_d(1 - H_f(z, h_c)), \quad (2)$$

where x and z are the streamwise and cross-stream (approximately surface normal) coordinates, respectively, with \bar{u} and \bar{w} the time averaged* velocities in the x and z directions, respectively, u' and w' are the corresponding turbulent velocity fluctuations, respectively, such that $\overline{u'} = \overline{w'} = 0$, $\bar{p}(x, z)$ is the mean static pressure (see Table I), and F_d is the canopy drag exerted by the vegetation on the air flow, which is parameterized as,

$$F_d = C_d a \bar{u}^2 \quad (3)$$

in which C_d is the dimensionless drag coefficient and $a(z)$ is the foliage area per unit volume. This foliage area is related to the (single sided) leaf area index (LAI) by

$$\text{LAI} = \int_{-h_c}^0 a(z) dz. \quad (4)$$

We take the origin of the cross-stream coordinate z at the top of the canopy. The term H_f is known as the Heaviside step function defined by

* Within the canopy, variables are also volume averaged over thin slabs containing many foliage elements to remove the large point-to-point variations in mean quantities within the canopy airspace (Brunet et al., 1994). The extra ‘dispersive’ flux terms that this volume averaging produces are absorbed in the Reynolds stresses. A recent study by Poggi et al. (2004b) suggests that these dispersive fluxes are small relative to the Reynolds stresses in dense canopies.

TABLE I
Parameters used in the model calculations.

Parameters	Values
<i>Site attributes</i>	
Latitude ($^{\circ}$ N), elevation (m)	35.8, 160
<i>Hill attributes</i>	
$Z = f(x)$ and $p(X)$	$Z = \frac{H}{2}(\cos(k'X) - 1) - h_c$ $p(X) = -\frac{U_o^2 H}{2k'} \cos(k'X)$ $k' = \frac{\pi}{2L}$
H (m), l (m)	20, 100
<i>Canopy attributes</i>	
LAI, Ω , x'	3.0, 0.8, 1 or spherical
$h_c(m)$, C_d	10, 0.2
<i>Physiological/respiration attributes</i>	
g_o (mol m $^{-2}$ leaf s $^{-1}$), a_1 , D_o (kPa), d' (m)	0.02, 4.4, 1.5, 0.015
T_a ($^{\circ}$ C) (assumed constant)	28.9
k_c , Γ^* , $V_{c,max}$ (μ mol m $^{-2}$ leaf s $^{-1}$)	403, 41, 64
$[O_2]$, K_o (mmol m $^{-2}$ leaf s $^{-1}$)	210, 322
R_E (μ mol m $^{-2}$ ground s $^{-1}$), $C_{surface}$ (ppm)	9.3, 450

Canopy physiological and respiration parameters are typical for the Duke Forest *Pinus taeda* stand, while the canopy height was set to 10 m (i.e. $h_c/H = 0.5$). The pressure variation is also shown with U_o being the outer layer velocity determined as in FB04.

$$H_f = \begin{cases} 1; & z > 0 \\ 0; & -h_c < z \leq 0 \end{cases} \quad (5)$$

Using first-order closure principles, $\overline{u'w'}$ is given by

$$\overline{u'w'} = -l_m^2 \left. \frac{\partial \bar{u}}{\partial z} \right| \left(\frac{\partial \bar{u}}{\partial z} \right), \quad (6)$$

where l_m is the mixing length, which is assumed constant within the canopy and increases linearly above the canopy (see Poggi et al., 2004a for a review). FB04 derived an analytical solution for the perturbations in \bar{u} , \bar{w} and $\overline{u'w'}$ caused by the hill for the case of constant $C_d a$ and H/L sufficiently small that the equations could be linearized and $\partial \overline{u'w'}/\partial x$ can be neglected. With \bar{u} given by the solution of Equation (2), \bar{w} can be computed from Equation (1).

The use of first-order closure models in canopy flows can be questioned on both theoretical and experimental grounds (Wilson and Shaw, 1977;

Denmead and Bradley, 1985; Finnigan, 1985; Albertson et al., 2001; Finnigan, 2000). FB04, however, show that, while such parameterization should be regarded as merely heuristic when applied to the mean flow, there is sound dynamical support for their use to describe the perturbations induced by the hill. On a practical note, Pinard and Wilson (2001) recently demonstrated that the skill of first-order closure models in reproducing \bar{u} is comparable to that of second-order closure models even for highly irregular leaf area density (on flat terrain). Notably, they compared their first-order closure model calculations to two higher order closure model calculations reported in Katul and Chang (1999) and found comparable root-mean-squared error between measurements and model calculations. Also, using a constant mixing length model inside the canopy, Poggi et al. (2004a) demonstrated that such first-order closure models reproduce well measured \bar{u} and $\overline{u'w'}$ within vertically arrayed rods in a flume for a wide range of roughness densities. A recent study by Katul et al. (2004) demonstrated that for six canopy types, first-order closure models with assumed constant l_m within the canopy space performed as well as standard $K - \varepsilon$ models (or 1.5-order closure models) in reproducing \bar{u} and $\overline{u'w'}$.

2.2. SCALAR MASS CONSERVATION

For steady state conditions, the conservation of the mean atmospheric CO₂ concentration, \bar{c} , is given by

$$\bar{u} \frac{\partial \bar{c}}{\partial x} + \bar{w} \frac{\partial \bar{c}}{\partial z} = - \left(\frac{\partial F_c}{\partial z} + \frac{\partial F_{cx}}{\partial x} \right) + S_c(1 - H_f(z, h_c)), \quad (7)$$

where $F_c = \overline{w'c'}$ and $F_{cx} = \overline{u'c'}$ are, respectively, cross-stream and streamwise turbulent fluxes of CO₂, and S_c is the source or sink of CO₂. Here, \bar{u} and \bar{w} are given by the solution to Equations (1) and (2). To close the problem, S_c , F_c , and F_{cx} , are made dependent on \bar{c} . For turbulent fluxes, a first-order closure model analogous to Equation (6) is used,

$$F_c = -K_c \frac{\partial \bar{c}}{\partial z}, \quad (8a)$$

$$F_{cx} = -K_c \frac{\partial \bar{c}}{\partial x}, \quad (8b)$$

where $K_c = l_m^2 \left| \frac{\partial \bar{u}}{\partial z} \right|$. In Equation (8), we assumed the turbulent diffusivity is isotropic.

To establish the relationship between S_c and \bar{c} we make use of ecophysiological principles as described next.

2.3. ECOPHYSIOLOGICAL CONTROLS ON CO₂ SOURCES AND SINKS

The transfer of CO₂ from the epidermis to the canopy airspace is assumed to be a Fickian diffusion process, written as

$$S_c = g_{\text{eff}} a(z) (\bar{c}_i - \bar{c}), \quad (9)$$

where g_{eff} is the effective conductance (per unit leaf area) for CO₂ transport from the sub-stomatal cavity to the canopy airspace, and \bar{c}_i is the mean intercellular CO₂ concentration; g_{eff} can be estimated from the boundary layer (g_b) and stomatal (g_s) conductances using:

$$\frac{1}{g_{\text{eff}}} = \frac{1}{g_s} + \frac{1}{g_b}. \quad (10)$$

For a laminar boundary layer on a leaf with characteristic length d' , g_b (in mol m⁻² s⁻¹) for CO₂ is given by

$$g_b = B \sqrt{\frac{\bar{u}}{d'}}, \quad (11)$$

where B depends inter alia, on leaf shape and ambient turbulence levels. For laminar flow parallel to a flat plate $B = 0.11$ but Finnigan and Raupach (1987) showed that for a leaf in the high ambient turbulence typical of the canopy airspace, a more appropriate value is $B = 0.22$ (and is used here).

The stomatal conductance g_s is dependent on net leaf photosynthesis (A_n) and can be parameterized using multiple semi-empirical formulations. Based on a recent study by Katul et al. (2000), we select the Leuning (1995) model because it best describes the stomatal respond to vapour pressure deficit (in the absence of soil moisture limitations on transpiration). It is given by

$$g_s = g_o + \frac{a_1 A_n}{\bar{c}_s - \Gamma^*} \left(1 + \frac{D_s}{D_o} \right)^{-1}, \quad (12)$$

where Γ^* is the CO₂ compensation point, \bar{c}_s is the mean surface CO₂ concentration, which can be related to \bar{c} using $\bar{c}_s = \bar{c} - \frac{A_n}{g_b}$, D_s is the mean surface vapour pressure deficit and g_o , a_1 and D_o are constants that vary among species. The \bar{c}_i term in Equation (9) is also related to A_n using the models of Farquhar et al. (1980) and Collatz et al. (1991), given by

$$A_n = \min \left\{ \begin{array}{l} \frac{\alpha_p Q_p e_m (\bar{c}_i - \Gamma^*)}{\bar{c}_i + 2\Gamma^*} - R_d \\ \frac{V_{c\text{max}} (C_i - \Gamma^*)}{\bar{c}_i + k_c \left(1 + \frac{\alpha_i}{k_o} \right)} - R_d \end{array} \right., \quad (13)$$

where α_p is the leaf absorptivity for the photosynthetically active radiation, PAR, e_m is the maximum quantum efficiency, and Q_p is the photosynthetically active irradiance. $V_{c\max}$ is the maximum catalytic capacity of Rubisco, k_c and k_o are the Michaelis constants for CO_2 fixation and O_2 inhibition with respect to CO_2 , o_i is the oxygen concentration, and $R_d = 0.015V_{c\max}$ is the respiration rate of the foliage. The latter coefficients vary with temperature as described in Lai et al. (2000).

Noting that $A_n = g_{\text{eff}}(\bar{c}_i - \bar{c})$, Equations (7)–(13) can be solved for \bar{c} , \bar{c}_i , g_{eff} , S_c , and F_c for appropriate boundary conditions and for a specified $Q_p(x, z)$. The latter quantity can be estimated from incident PAR and a radiative transfer scheme described below. Two boundary conditions must be specified to solve Equation (7), viz.:

$$z = l_i, \bar{c} = C_o, \quad (14a)$$

$$z = -h_c; \begin{cases} -K_c \frac{\partial \bar{c}}{\partial z} = R_E(x) \text{ (flux boundary condition)} \\ \text{or } \bar{c} = C_{\text{surface}} \text{ (concentration boundary condition),} \end{cases} \quad (14b)$$

where C_o is the outer region concentration, assumed to be constant and independent of x , $R_E(x)$ is the forest-floor respiration that varies with temperature (Table I) and C_{surface} is the CO_2 concentration near the forest floor. We explore both types of boundary conditions by either specifying the forest floor flux or near surface concentration – both assumed constant with respect to the longitudinal distance across the hill length. In practice, this assumption is unrealistic as both forest floor flux and C_{surface} are likely to vary with litter depth and below-ground respiring biomass, soil moisture, and soil temperature, which are known to vary spatially across a hill. However, by imposing a lower-boundary condition (flux or mean surface concentration) that is constant with respect to x ensures that all the modelled F_c spatial variability is strictly produced from the interplay between the flow dynamics, radiative transfer, and nonlinear ecophysiological processes, the objective of this effort.

2.4. RADIATIVE TRANSFER

The spatial and temporal variation in Q_p is required to compute A_n . Campbell and Norman (1998) state that the vertical attenuation of incident radiation $Q_p(0, x)$ through the canopy is given by

$$\frac{Q_p(z, x)}{Q_p(0, x)} \approx \tau_b(z) = \exp(-\Omega K_b(x', \psi) L_t(z)), \quad (15)$$

where τ_b is the fractional amount of light arriving at depth z within the canopy, K_b is the extinction coefficient, which depends on the zenith angle

(ψ), x' is the ratio of average projected areas of canopy elements onto horizontal and vertical surfaces, Ω is the clumping factor, and $L_t(z) = \int_0^z a(z) dz$, where $-h_c < z \leq 0$. Assuming azimuthal symmetry in leaf area distribution, $K_b(x', \psi)$ for vegetation with an ellipsoidal leaf angle distribution is given by

$$K_b(x', \psi) \approx \frac{\sqrt{x'^2 + \tan^2(\psi)}}{x' + 1.774(x' + 1.182)^{-0.733}}. \quad (16)$$

For spherical, vertical, and horizontal leaf angle distributions, $x' = 1, 0$, and ∞ , respectively. Variation in $Q_p(0, x)$ across the hill is a function of the solar elevation angle (ψ_e), the azimuth angle (ψ_a), and the local hill slope ($\alpha(x)$). Raupach et al. (1992) showed that

$$\frac{Q_p(0, x) - Q_p(0, 0)}{Q_p(0, 0)} = -\cot(\psi_e) \cos(\psi_a) \sin(\alpha) + \cos(\alpha) - 1. \quad (17)$$

Equations (7)–(17) can be solved numerically as described in the Appendix A.

3. Results and Discussion

To assess how topography alters the spatial distribution of photosynthesis and F_c , the model described above is first applied to a gentle hill ($H = 20$ m, $L = 100$ m) with the hill affecting both radiative forcing and flow dynamics. Next, the model calculations are repeated for flat terrain ($H = 0$) using identical radiative and canopy drag attributes and ecophysiological parameters. Two other ‘intermediate’ hypothetical scenarios are also considered to address the study objective – the case in which the hill only affects the radiative forcing assuming the flow dynamics are identical to their flat terrain counterpart, and the case in which the hill only alters the flow dynamics assuming the incident radiative load above the canopy is constant across the hill. These cases are summarized in Table II with case 1 being the flat terrain scenario, case 2 being the scenario in which the effect of the hill only acts on the radiative perturbation with the flow dynamics retained from case 1, case 3 being the scenario in which the hill only acts on the flow dynamics with the radiative regime taken from case 1 and case 4 being the scenario in which the hill affects both – radiative regime and flow dynamics. As a case study, we use published ecophysiological, respiration, and drag properties from the Duke pine forest Ameriflux site (see Katul and Chang, 1999; Katul et al., 2000; Lai et al., 2000, 2002), which are summarized in Table I.

We begin by quantifying how the hill alters the key forcing variables (mean wind field and incident radiation) from their planar homogeneous state. Next, using these forcing variables, we discuss how the hill alters

TABLE II

Assessing the influence of momentum transfer, radiative forcing, and scalar mass balance on describing F_c and bulk canopy photosynthesis from a forest on a hill.

Case #	Momentum balance	Radiative forcing	Scalar mass balance
1.	$\bar{u} = U_b, \bar{w} = 0$ (flat terrain)	$\frac{\partial Q_p(0, x)}{\partial x} = 0$	$S_c = \frac{dF_c}{dz}$ (flat terrain).
2.	$\bar{u} = U_b, \bar{w} = 0$ (flat terrain)	$\left \frac{\partial Q_p(0, x)}{\partial x} \right \geq 0$	$S_c = \frac{dF_c}{dz}$ (radiation varied advection neglected).
3.	$\frac{\partial \bar{u}}{\partial x}, \frac{\partial \bar{w}}{\partial z}$ solved from Equation (1)	$\frac{\partial Q_p(0, x)}{\partial x} = 0$	$S_c = \frac{dF_c}{dz} + \frac{dF_c}{dx} + \bar{w} \frac{\partial \bar{C}}{\partial z} + \bar{u} \frac{\partial \bar{C}}{\partial x}$
4.	$\frac{\partial \bar{u}}{\partial x}, \frac{\partial \bar{w}}{\partial z}$ solved from Equation (1)	$\left \frac{\partial Q_p(0, x)}{\partial x} \right \geq 0$	$S_c = \frac{dF_c}{dz} + \frac{dF_c}{dx} + \bar{w} \frac{\partial \bar{C}}{\partial z} + \bar{u} \frac{\partial \bar{C}}{\partial x}$

The model formulation below are applied to mean meteorological conditions at 1430 and for $u_* = 0.4 \text{ m s}^{-1}$. Cases 1 and 4 represent the two end members, (i.e. flat and hilly terrain), in which the spatial variability in momentum balance, radiative forcing, and scalar mass balance control the spatial variability in S_c .

the mean scalar mass balance. The mean meteorological conditions (e.g. vapour pressure and air temperature) from a 30-min run around 1430 local time (high PAR but not constant in x) are used for illustration.

3.1. GENERATION OF THE FLOW FIELD

FB04 derived an approximate analytical solution for \bar{u} by decomposing the mean velocity into a background value and a perturbation introduced by the hill to give,

$$\bar{u}(x, z) = \bar{U}_b(x, z) + \Delta \bar{u}(x, z), \quad (18)$$

where \bar{U}_b is the background velocity prior to the air flow encountering the hill (and assumed to be identical to the mean velocity profile on a flat terrain), and Δu is the hill-induced perturbation in mean velocity. The FB04 solution applies in the limit $H/L \ll 1$ (as is the case here).

The background velocity can be adequately described by (Massman and Weil, 1999),

$$\bar{U}_b = U_h \exp\left(\frac{\beta z}{l_m}\right) \quad (19a)$$

for $-h_c < z < 0$,

$$\overline{U}_b = \frac{u_*}{\kappa} \ln \left[\frac{z+d}{z_0} \right] \quad (19b)$$

for $0 < z < l_i$, where, $U_h = \overline{U}_b(0)$ is the velocity at the top of the canopy, u_* is the background friction velocity, $\kappa = 0.4$ is von Karman's constant, z_0 is the aerodynamic roughness length and d the zero-plane displacement of the undisturbed flow.

Defining $\beta = u_*/U_h$ to represent the momentum flux through the canopy, its value is shown to be $\beta \approx 1/3$ for closed (and dense) uniform canopies as discussed in Raupach et al. (1996), Katul et al. (1998), and Finnigan (2000). By matching velocity and shear stress at the top of the canopy, FB04 find that

$$U_h = \frac{u_*}{\kappa} \ln \left[\frac{d}{z_0} \right], \quad (20a)$$

$$z_0 = d \exp \left(\frac{-\kappa}{\beta} \right), \quad (20b)$$

$$d = \frac{l_m}{\kappa}. \quad (20c)$$

For the within canopy flow, $l_m = 2\beta^3 L_c$ and varies with the canopy adjustment length $L_c = (C_d a)^{-1}$ (Belcher et al., 2003), where $a = \text{LAI}/h_c$. The mixing length needed for describing the eddy-diffusivity can be computed for a given LAI, h_c and C_d .

The depth of the inner region, l_i , is derived by matching the advection-distortion time scale with the turbulent relaxation time scale to give the implicit equation (Hunt et al., 1988),

$$\frac{l_i}{L} \ln \left(\frac{l_i}{z_0} \right) = 2\kappa^2. \quad (21)$$

The application of Equation (20) may not be precise, as discussed in Physick and Garratt (1995); however, it is sufficiently accurate for the purposes of computing mean longitudinal velocity perturbations induced by the hill in the context of scalar transport and neutral flows. For example, the modelled background (horizontally homogeneous) mean velocity is shown in Figure 2 for a constant leaf area density profile, $a = \text{LAI}/h_c$ with $\text{LAI} = 3$, $h_c = 12$ m, and $C_d = 0.2$ so that $L_c \approx 20$ m and $l_m \approx 1.5$ m. For reference, the measured mean velocity profile at the Duke pine stand, reported in Katul and Chang (1999), for the same LAI, h_c and C_d are also shown. While the measured leaf area density profile at Duke Forest is far from constant (Katul and Chang,

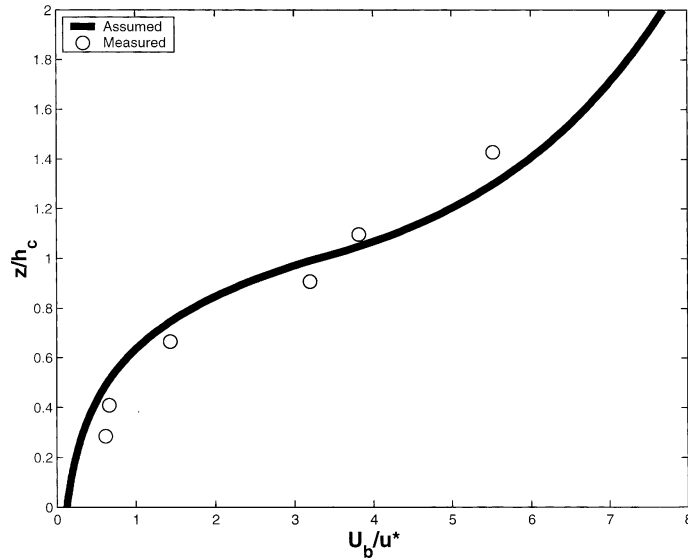


Figure 2. Variation of the normalized background velocity (U_b) with normalized height (z). Here, U_b is normalized by the friction velocity (u_*) at the top of the canopy, and z is normalized by the canopy height (h_c). For reference, measured velocity reported in Katul and Chang (1999) from a pine forest with comparable h_c and LAI are shown (circles).

1999), the modelled $\overline{U_b}$ reproduces the measured mean velocity profile quite well. Evidently the $\overline{U_b}$ formulation is insensitive to the precise distribution of leaf area density (at least in dense canopies).

A key feature of the FB04 model for Δu is the asymptotic division of the canopy into two layers with distinctly different dynamics. In the upper canopy, the momentum balance is between the streamwise pressure gradient, the shear stress divergence and the canopy drag, while in the lower canopy the dynamic balance involves only the pressure gradient and the drag (i.e. the shear stress divergence is negligible for the deeper layers of dense canopies). The computed $\Delta \overline{u}$ for the hill geometry of Figure 1 with $H = 20$ m and $L = 100$ m has three characteristics (that are independent of u_*) as shown in Figure 3:

1. On the upwind side of the hill, $\Delta \overline{u}$ within the lower canopy layer increases up to $x = -L$ and then decreases, passing through zero on the hillcrest and reaching its maximum negative value at $x = +L$ on the downwind slope.
2. The maximum $\Delta \overline{u}$ above the canopy occurs just in front of the hillcrest at $x = 0$ and this maximum is out of phase with the maxima in $|\Delta \overline{w}|$, which occur at $x = \pm L$.
3. The negative value of $\Delta \overline{u}$ within the deeper layers of the canopy on the downwind slope exceeds $\overline{U_b}$ and is sufficient to reverse the total airflow

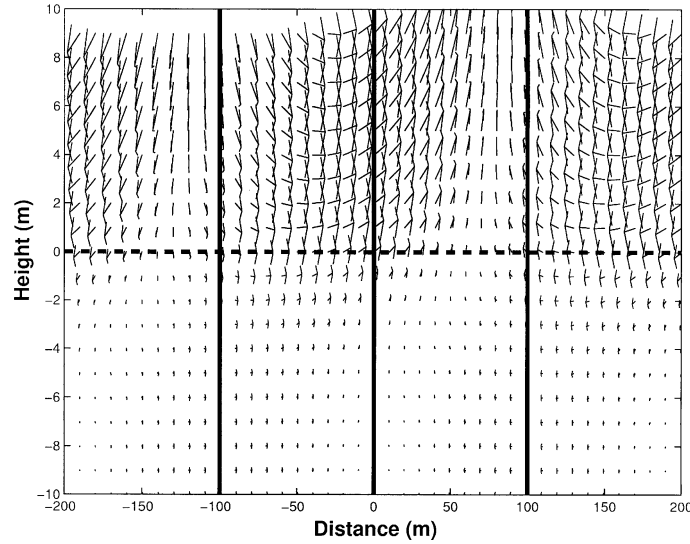


Figure 3. A quiver plot of the wind vector perturbations Δu and Δw for the hill geometry shown in Figure 1 and the U_b in Figure 2. The horizontal line defines the canopy top. The vertical lines are locations of ‘virtual towers’ used to investigate the profiles of the scalar mass budget from the model at $x = -L$, 0 , and $+L$.

($\bar{u} = \bar{U}_b + \Delta\bar{u} < 0$) and to set-up a ‘recirculation region’. This circulation significantly distorts the symmetry of the mean flow and all attendant mean quantities* about the hillcrest $x = 0$. The extent of the recirculating region is best illustrated by the streamlines of the *total* flow shown in Figure 4 (see Figure 7a in FBO4 for further details).

We note that the mean CO_2 mass balance is likely to be very sensitive to such asymmetry. Small spatial gradients in mean CO_2 concentration acted upon by a moderate mean velocity can lead to advection terms $\bar{u}\partial\bar{c}/\partial x$ or $\bar{w}\partial\bar{c}/\partial z$ whose individual numerical values may exceed midday leaf photosynthesis. For example, a $\partial\bar{c}/\partial x \approx 0.1 \text{ ppm m}^{-1}$ acted upon a $\bar{u} = 1 \text{ m s}^{-1}$ ($\approx 4.14 \mu\text{mol m}^{-3}\text{s}^{-1}$) is comparable to a leaf photosynthesis of about $17 \mu\text{mol m}^{-2}\text{s}^{-1}$ for a 12-m tall canopy with an $LAI = 3 \text{ m}^2 \text{ m}^{-2}$ ($\approx 4.25 \mu\text{mol m}^{-3}\text{s}^{-1}$). Note that for the maturing loblolly pine forest of the Duke Ameriflux site, midday leaf photosynthesis of the upper layers sunlit foliage is on the order of $15 \mu\text{mol m}^{-2}\text{s}^{-1}$ (Katul et al., 2000). Hence, given the horizontal variability in mean flow, we anticipate that the individual advective terms are likely to be key contributors to the overall budget of forest-atmosphere CO_2 exchange.

* To generate the flow field used in these calculations we use a linearized version of the full non-linear FBO4 solution for the deep canopy. This linearized solution produces a somewhat smaller flow asymmetry than the full non-linear solution.

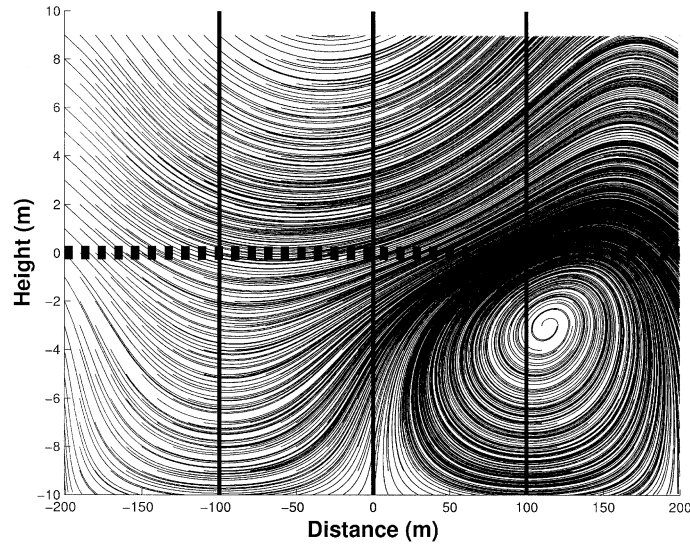


Figure 4. Lagrangian trajectories of the mean velocity (\bar{u} and \bar{w}) for the hill geometry shown in Figure 1 illustrating the extent of the recirculation region. The horizontal line defines the canopy top; the vertical lines are as in Figure 3.

3.2. RADIATIVE TRANSFER

Another source of horizontal variability in S_c is incident photosynthetically active radiation at the canopy top $Q_p(0, x)$, which varies with solar declination, azimuth, and local topographic slope. Using the sunrise convention in Figure 1 and Equation (17), we compute $Q_p(0, x)$ for different hours of the day to illustrate its magnitude (Figure 5). $Q_p(0, x)$ across the hill varies between -6% and 3% from 0830 to 1430, with opposite symmetry in the afternoon. We note that since $Q_p(0, x)$ only influences the light-limited photosynthesis rate, the total canopy photosynthesis will, in fact, be influenced by much less than the 10% variation in radiation early in the morning and late afternoon. Spatial variation in photosynthesis is even less around midday. Hence, based on the results in Figure 5, we do not anticipate that the horizontal variation in $Q_p(0, x)$ will be a key factor though we retain it in the analysis of cases 2 and 4 for reference.

Next we describe how the spatial variability in $\Delta\bar{u}$, $\Delta\bar{w}$, and $Q_p(0, x)$ affect the components of the mean scalar budget (i.e. cases 2, 3, and 4 in Table II).

3.3. MEAN SCALAR MASS BALANCE

Using the parameters in Table I, the mean scalar mass balance is solved for two types of the lower boundary condition (i.e. two solutions):

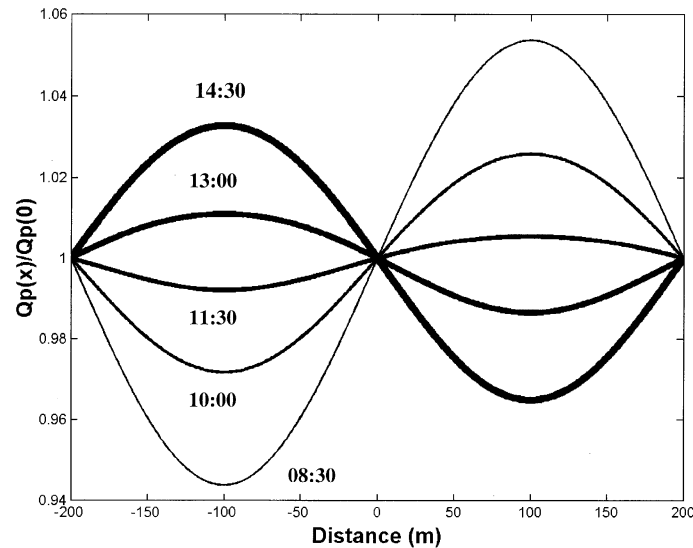


Figure 5. The relative variation of the incident photosynthetically active radiation (Q_p) at the canopy top ($z = 0$) as induced by the hill geometry for various hours during the day. The sunrise convention relative to the hill is shown in Figure 1.

concentration with $C_{\text{surface}} = 450$ ppm, and respiration $R_E = 9.3 \mu\text{mol m}^{-2} \text{s}^{-1}$. The R_E value was determined from air temperature measurements.

The leftmost panels in Figure 6 show the modelled forcing variables (mean horizontal and vertical wind fields and photosynthetically active radiation), while the other panels show the response variables (mean CO_2 concentration, photosynthesis and CO_2 fluxes) for 1430 local time. At this time, photosynthesis is large and $Q_p(0, x)$ is not constant (Figure 5). The middle panels are results obtained using a constant flux boundary condition at the soil surface, while the rightmost panels are for the constant concentration boundary condition.

Several things are evident from Figure 6. First, the overall spatial patterns of the response variables \bar{c} , S_c and F_c are insensitive to the lower boundary conditions. Second, while the proportional variation in modelled S_c is much smaller than H/L , the proportional variability in F_c is at least an order of magnitude larger than H/L . Third, the value of $\partial\bar{c}/\partial x$ across the hill, especially near the hilltop and within the recirculating region, is much larger than 1 ppm per 10 m suggesting that the advection terms are major components of the budget of scalar transport.

We explore the relative importance of these terms at three 'hypothetical towers' positioned at $x = -L, 0, +L$ (see Figures 1, 4), representative of upwind, hilltop, and downwind conditions. The profiles of the forcing and response variables and their relationship to the components of the

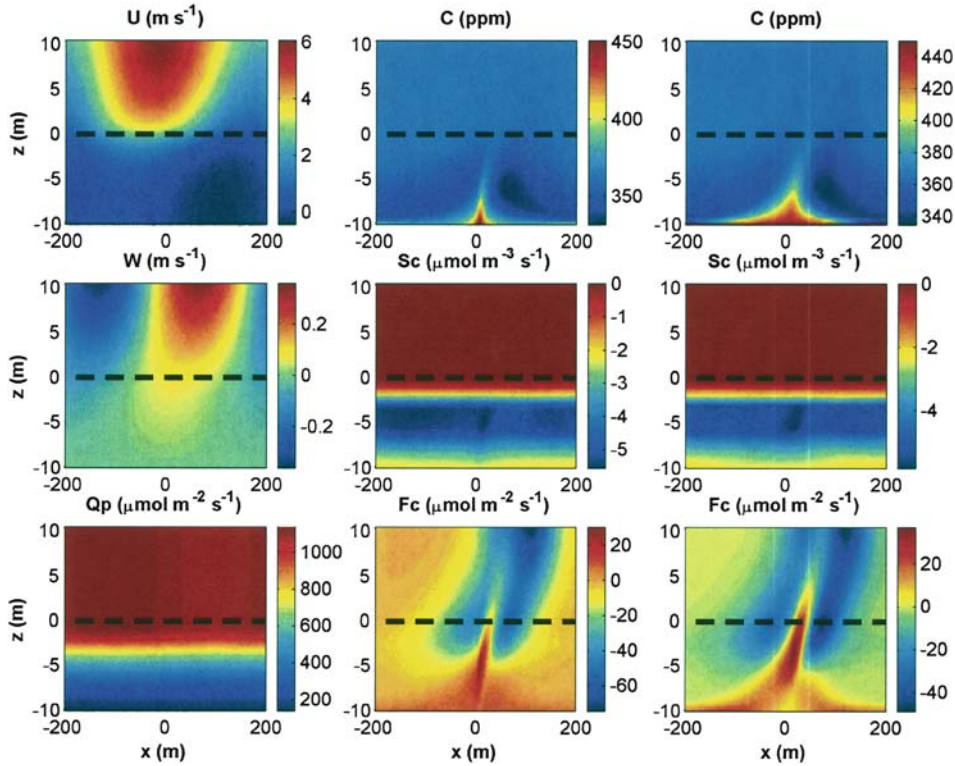


Figure 6. Spatial variation of the forcing (left panels) and response variables for flux (middle panels) and concentration (right panels) boundary conditions. The forcing variables include the mean wind field (\bar{u} , \bar{w}) and incident photosynthetically active radiation (Q_p) and the response variables include mean CO_2 concentration (\bar{c}), above ground CO_2 sources and sinks (S_c), and the turbulent CO_2 fluxes ($F_c = \overline{w'c'}$). For reference, the canopy top is shown as a dashed horizontal line. The model calculations are for steady-state neutral flows.

scalar mass balance at these positions (as might be measured from a flux-monitoring tower) are shown in Figure 7 for the two lower boundary conditions. Figure 7 shows that the CO_2 concentration and fluxes vary appreciably between the three towers and significantly depart from their counterparts over ‘flat-terrain’. The computations show that at $x=0$ and at $x=-L$, F_c above the canopy has the opposite sign compared to the flat terrain case, while at $x=+L$, F_c is far more negative. This figure also shows that there is no tendency for the computed fluxes to converge to the flat terrain case with increasing height above the hill. Since the variation in $Q_p(x, 0)$, S_c and g_{eff} are small, the large excursions in F_c from their flat terrain counterparts cannot be attributed to variability in photosynthesis, but instead are the result of flow distortions induced by the hill.

Figure 8 shows the modelled components of the mass balance at these three tower locations: the divergence in horizontal and vertical turbulent

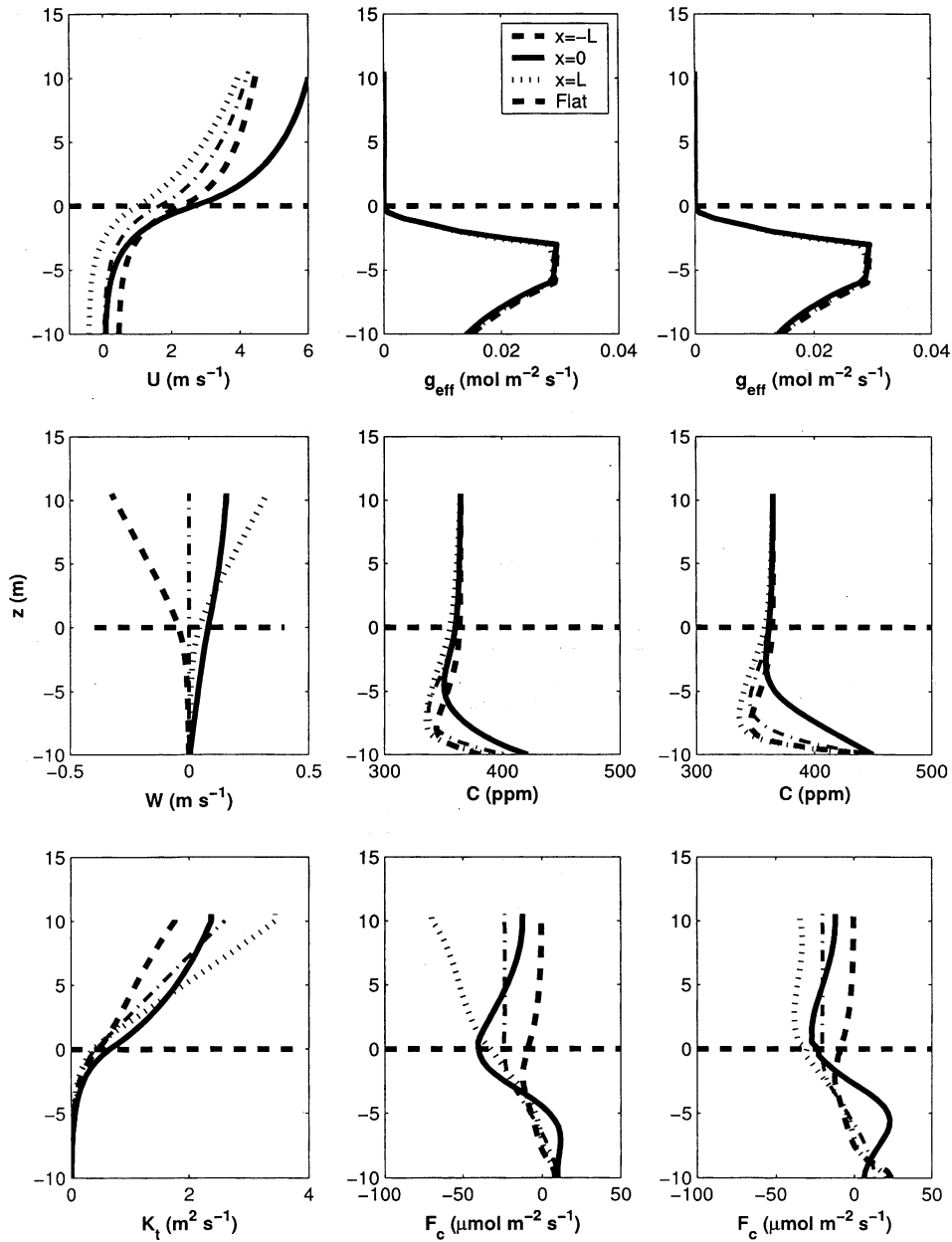


Figure 7. The profiles of the forcing (left panels) and response variables for flux (middle panels) and concentration (right panels) boundary conditions at $x=-L$, $x=0$, and $x=+L$. For reference, the profiles for the flat terrain case (i.e. $H=0$) are also shown. The model calculations are for steady-state neutral flows.

fluxes, the two advection terms and the biological sources and sinks. The same quantities for the flat terrain case are also shown for reference. Figure 8 corresponds to the flux boundary conditions at the soil surface (the concentration boundary conditions were qualitatively similar). The calculations demonstrate that within the canopy on a hill, the vertical turbulent flux divergence term $|\partial F_c/\partial z|$ does not match the source term $|S_c|$ (i.e. $\partial F_c(z)/\partial z \neq S_c(z)$) and above the canopy $\partial F_c/\partial z \neq 0$. This contrasts with the flat terrain case, where $\partial F_c(z)/\partial z = S_c(z)$ and $\partial F_c/\partial z = 0$ within and above the canopy, respectively. The imbalance between $|\partial F_c/\partial z|$ and $|S_c|$ is redressed by the remaining terms in the scalar balance in Equation (7), expressed as the quantity $\phi = \bar{u}\partial\bar{c}/\partial x + \bar{w}\partial\bar{c}/\partial z + \partial F_{cx}/\partial x$ at all three positions. In homogeneous flow over flat terrain, note that $\phi = 0$.

Among the three components of ϕ , Figure 8 further suggests that the horizontal turbulent flux divergence term, $|\partial F_{cx}/\partial x|$, is an order of magnitude smaller than $\bar{u}\partial\bar{c}/\partial x$ and so the imbalance between $\bar{u}\partial\bar{c}/\partial x$ and $\bar{w}\partial\bar{c}/\partial z$ is the primary contributor to the imbalance between $|\partial F_c/\partial z|$ and $|S_c|$. In short, the local flux gradient is decoupled from the local photosynthesis at those positions because $\bar{u}\partial\bar{c}/\partial x$ and $\bar{w}\partial\bar{c}/\partial z$ are not locally and precisely in balance. Figure 8 also demonstrates that $\bar{u}\partial\bar{c}/\partial x$ and $\bar{w}\partial\bar{c}/\partial z$ individually are much larger than $|S_c|$ (by a factor of three in certain regions of the flow domain), and, hence, a minor imbalance between them results in a substantial difference between $|\partial F_c/\partial z|$ and $|S_c|$. These model results highlight another challenge to inferring biological sources and sinks of CO_2 from single flux tower measurements: the terms $\bar{u}\partial\bar{c}/\partial x$ and $\bar{w}\partial\bar{c}/\partial z$ are of the same order of magnitude but opposite in sign. While $\bar{w}\partial\bar{c}/\partial z$ may be estimated from single tower measurements, $\bar{u}\partial\bar{c}/\partial x$ may not. The fact that $\bar{u}\partial\bar{c}/\partial x$ and $\bar{w}\partial\bar{c}/\partial z$ are comparable means that both terms must be considered simultaneously in any analysis relating $\partial F_c/\partial z$ and S_c . In an inviscid flow without scalar diffusion, variations in the scalar fields would be caused purely by advection and $\bar{u}\partial\bar{c}/\partial x$ and $\bar{w}\partial\bar{c}/\partial z$ would precisely cancel each other (Raupach et al., 1992). Within the region $z < l_i$, where turbulent stresses and scalar eddy fluxes are important, however, perturbations to the eddy covariance fluxes caused by the topography interact with the velocity perturbations to break this symmetry. The recirculating region (Figure 4) further compounds the problem because it exaggerates asymmetry in the imbalance between $\bar{u}\partial\bar{c}/\partial x$ and $\bar{w}\partial\bar{c}/\partial z$, leading to variations in F_c with position above the canopy. With few exceptions, instruments on flux towers in complex topography over tall vegetation are located in this inner region $z < l_i$ and so the inference of biological sources and sinks computed from turbulent fluxes are liable to significant error due to the advection terms. An immediate consequence of the asymmetry between $\bar{u}\partial\bar{c}/\partial x$ and $\bar{w}\partial\bar{c}/\partial z$ is that the imbalance between $\partial F_c/\partial z$ and S_c will be highly sensitive to wind direction even when all

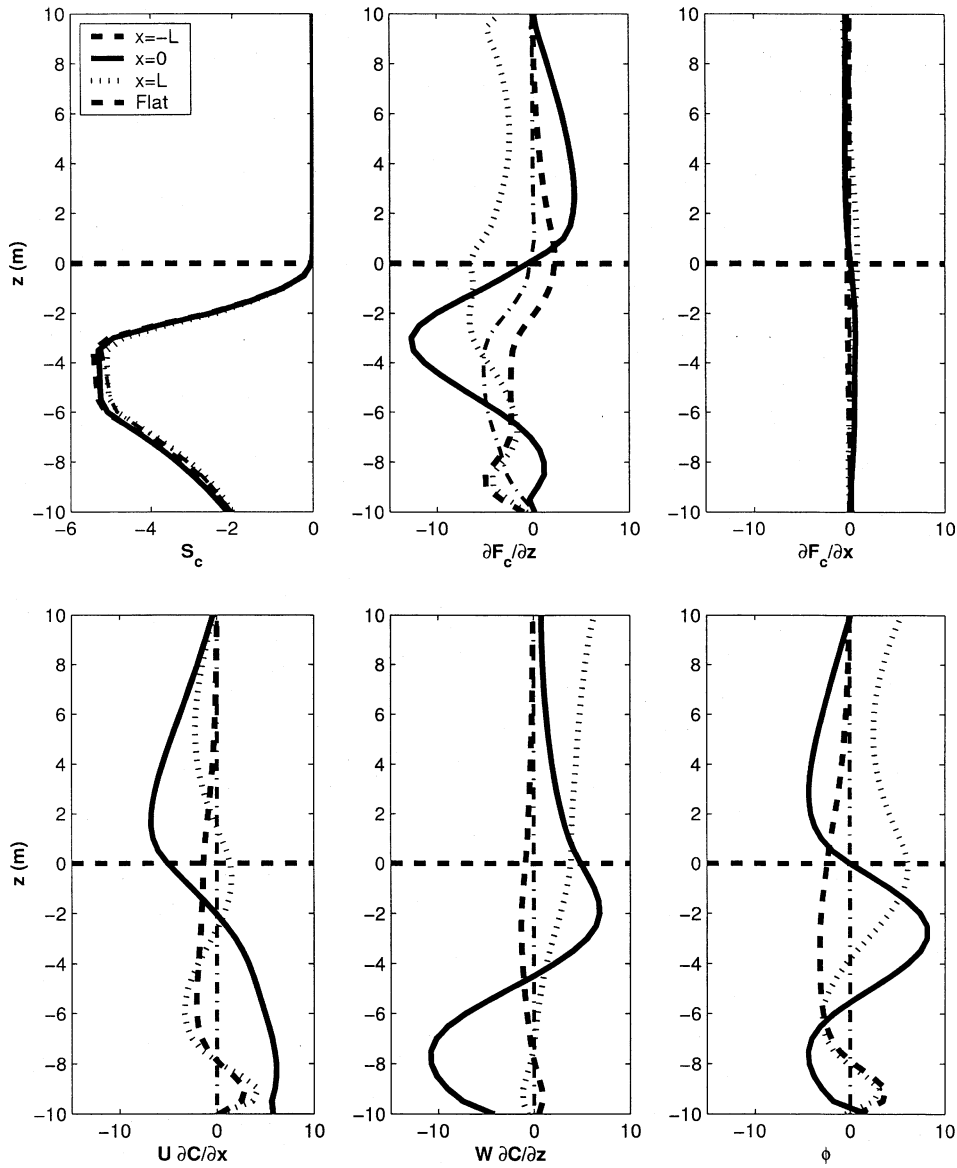


Figure 8. The components of the scalar mass balance (in $\mu\text{mol m}^{-3} \text{s}^{-1}$) for the flux boundary condition at $x = -L$, $x = 0$, and $x = +L$. The variable $\phi = \bar{u}\partial\bar{c}/\partial x + \bar{w}\partial\bar{c}/\partial z + \partial F_c/\partial x$ is the imbalance between S_c and dF_c/dz . For a flat terrain ($H = 0$), $S_c = dF_c/dz$, and $\phi = 0$. For reference, the flat terrain profiles are also shown; the model calculations are for steady-state neutral flows.

other parameters remain identical. These model results are in qualitative agreement with recent field experiments conducted in Tharandt, Germany in which the horizontal advection and vertical advection were found to be comparable, opposite in sign, and larger than the daytime photosynthesis (Feigenwinter et al., 2004).

We conducted the same calculation for the midnight run and found that $\bar{u}\partial\bar{c}/\partial x$ and $\bar{w}\partial\bar{c}/\partial z$ are comparable in magnitude and both are much larger than $|S_c|$ (as expected) and that $\partial F_c/\partial z$ is primarily controlled by ϕ .

The next step is to investigate how the components of the mass balance integrated through the depth of the canopy depart from their flat-terrain counterparts.

3.4. EFFECT OF TOPOGRAPHY ON CANOPY-AVERAGED PHOTOSYNTHESIS AND MASS BALANCE

The depth-integrated scalar mass balance can be expressed as:

$$\int_{-h_c}^0 S_c(z, x) dz = F_c(0, x) - R_E(-h_c, x) + \int_{-h_c}^0 \phi(z, x) dz,$$

where $\int_{-h_c}^0 S_c(z, x) dz$ is the total canopy photosynthesis, $F_c(0, x)$ is the turbulent flux measured by the eddy-covariance system at the canopy top, $R_E = F_c(-h_c, x)$ is respiration from the forest floor, and $\int_{-h_c}^0 \phi(z, x) dz$ is the depth-integrated advective fluxes. In Figure 9 (left panels), we present the variation with x of these individual components, while the right panels in Figure 9 show separately F_c , R_E and the components of ϕ . The calculations are for the flux boundary conditions at 1430 hours and we note that the concentration boundary conditions were qualitatively similar.

Bulk Canopy Photosynthesis: From Figure 9, we find that canopy photosynthesis peaks behind the hillcrest exceeding its flat terrain value of $\approx 34 \mu\text{mol m}^{-2} \text{s}^{-1}$ by about $3 \mu\text{mol m}^{-2} \text{s}^{-1}$. The average canopy photosynthesis across the hill (along x) is also shown for comparison with the flat land counterpart so as to assess the total effect of the distortion of the wind field and radiation input by the hill. We find the overall canopy photosynthesis increases by $\approx 3\%$ because of the presence of the hill, which is much smaller than the hill slope, H/L , of 20%. This is not surprising as photosynthesis in this set-up is primarily governed by stomatal, not boundary-layer conductance.

Turbulent Flux: In contrast, we find large variations in the turbulent flux across the hill. As foreshadowed in Figure 8, the large positive excursion in F_c just behind the crest is of the same order as the depth-averaged canopy photosynthesis we wish to measure. Indeed, a tower located just behind the crest and measuring only F_c would indicate the canopy

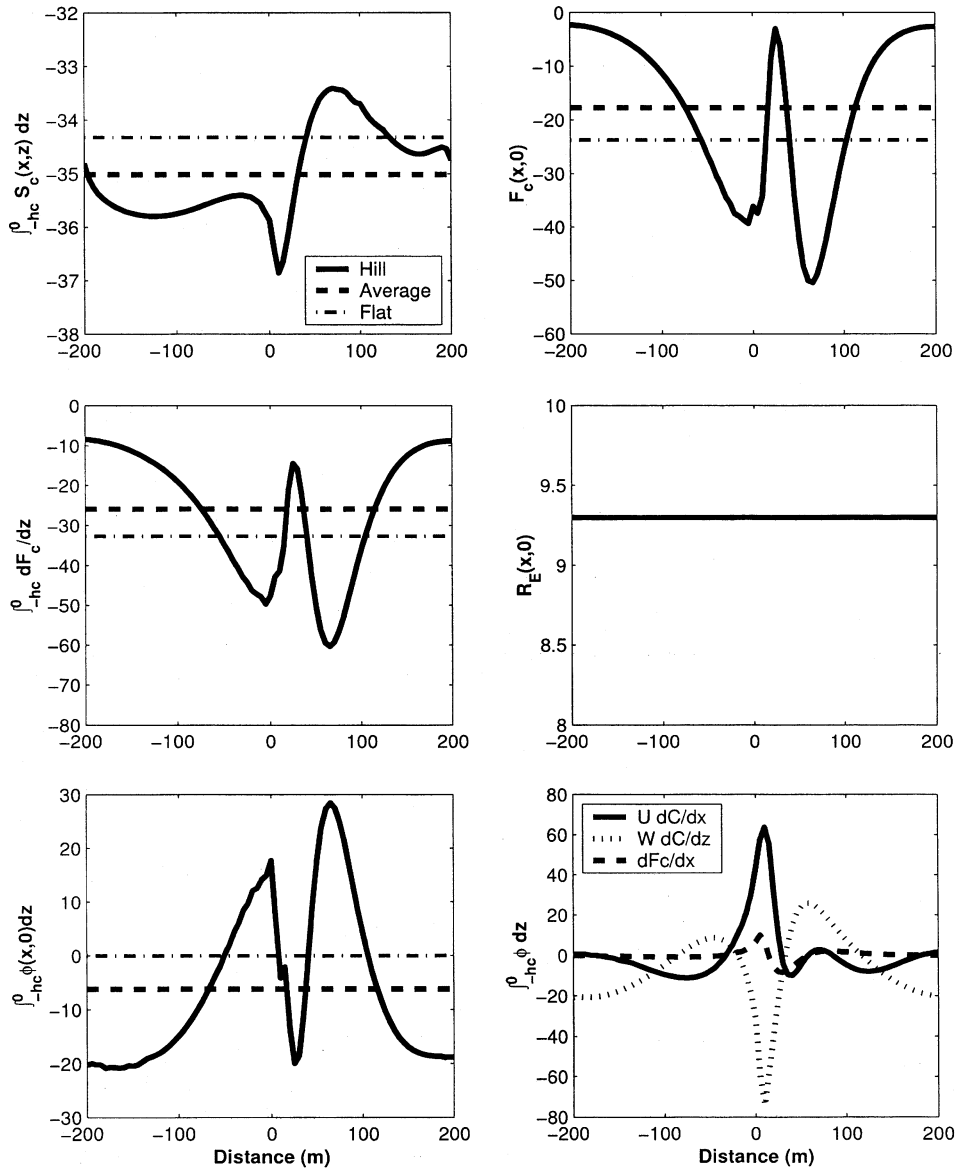


Figure 9. Horizontal variation of the components (in $\mu\text{mol m}^{-2} \text{s}^{-1}$) of the integrated scalar mass balance (left columns) for the flux boundary condition. The right panels show the components contributing to $\int_{-hc}^0 (dF_c/dz) dz$ (top right and middle) and $\int_{-hc}^0 \phi(x,0) dz$ (bottom right). The flat terrain values are shown for reference; the model calculations are for steady-state neutral flows.

was nearly ‘carbon neutral’ rather than a vigorously photosynthesizing pine forest. This reduction in CO_2 flux into the canopy just behind the crest appears to be spatially connected with the tongue of air carried out of the canopy by the re-circulation region (see Figure 4) and appears persistent in both boundary conditions. If so, this reduction in CO_2 turbulent flux into the canopy just behind the crest is likely to be a canonical feature of the flow dynamics.

Finally, we see that the average of F_c across the hill is smaller than its flat land counterpart by about $5 \mu\text{mol m}^{-2} \text{s}^{-1}$. The difference between the average F_c across the hill and the flat terrain F_c is of order of the hill slope (H/L). The genesis of this F_c difference is explored next.

Advection Terms: The bottom panels in Figure 9 display the remaining components of the height-integrated mass balance, which are collected in the term ϕ . The bottom right panel shows the two advection terms and the horizontal gradient of the horizontal eddy-flux, $\partial \overline{u'c'}/\partial x$, which is an order of magnitude smaller than either of the two advection terms (for both boundary conditions). There are large excursions in both advection terms just behind the hillcrest, and peak at values nearly double the magnitude of the canopy photosynthesis. It is clear from Figure 9 that the departure of F_c from the flat terrain values is a result of the advective transport terms. Moreover, a breakdown in symmetry within the concentration field (Figure 6) clearly leads to a systematic bias in $\int_{-h_c}^0 \phi(x, z) dz$. For example, the horizontal average of $\int_{-h_c}^0 \phi(x, z) dz$ across the hill remains some 25% of the magnitude of F_c over flat terrain for the constant flux boundary condition. In Table III, we further investigate this point by assessing how the different simplifications to the mean momentum and scalar mass balance in Table II affect the ratio

TABLE III

The variation of B_H for the two types of boundary conditions and for all four cases.

Time	Case no.	B_H	
		FLUX BC	CONC. BC
1430	1	1.0	1.0
	2	0.99	0.99
	3	0.82	0.89
	4	0.81	0.90

$$B_H = \frac{\langle F_c(x, 0) \rangle - \langle R_E \rangle}{\int_{-h_c}^0 S_c(x, z) dz|_{H=0}},$$

where the spatial averaging operator $\langle \zeta \rangle$ is defined as

$$\langle \zeta \rangle \equiv \frac{1}{4L} \int_{-2L}^{2L} \zeta(z, x) dx.$$

Again, Table III clearly suggests that the primary mechanism responsible for the departure of B_H from unity is not horizontal variation in radiation (case 2) but is caused by flow dynamics and advection transport terms. Another interesting point is that for case 4, B_H for the flux boundary condition is smaller than its counterpart for the concentration boundary condition.

4. Conclusions

We present a first-order closure model of the effect of gentle hills ($H/L \leq 0.2$) on forest-atmosphere CO_2 exchange for the most idealized conditions: well-watered uniform vegetation embedded in a non-stratified, high Reynolds number flow on a cosine-shaped hill (i.e. one Fourier mode of variability in the terrain). Using this model, we found the following:

1. Streamwise variations in \bar{u} and \bar{w} induced by the hill are out of phase in the upper canopy and in the surface layer ($z < l_i$) and are asymmetric about the hill top, $x = 0$. Deep within the canopy this asymmetry results in a recirculation region in the lee of the hill.
2. The fractional error in modelling total photosynthesis of a forest on a hill by ignoring all topographic variation in radiation is much smaller than H/L .
3. The advection terms $\bar{u}\partial\bar{c}/\partial x$ and $\bar{w}\partial\bar{c}/\partial z$ are individually much larger than the sink term S_c at many positions within the canopy and across the hill. Model calculations suggest that $\bar{u}\partial\bar{c}/\partial x$ and $\bar{w}\partial\bar{c}/\partial z$ are usually opposite in sign but do not precisely cancel each other locally or even when averaged across the hill. This leads to strong variations of the vertical turbulent flux $F_c = \overline{w'c'}$ with position across the hill. The lack of cancellation of $\bar{u}\partial\bar{c}/\partial x + \bar{w}\partial\bar{c}/\partial z$ results in persistent patterns such as the reduction in CO_2 flux into the canopy just behind the crest of the hill. This persistent pattern is attributed to air carried out of the canopy volume by the re-circulating region at the lee side of the hill as previously discussed.

The broader implication of these conclusions is that the effects of topography can be ignored when modelling forest photosynthesis on gentle hills, but the same simplification is not valid when inferring CO₂ fluxes from tower measurements. The imbalance between $\bar{u}\partial\bar{c}/\partial x$ and $\bar{w}\partial\bar{c}/\partial z$ is sufficiently large to decouple the local canopy photosynthesis from the local turbulent flux. Hence, linking tower-based eddy-covariance measurements to local biological sources and sinks on hilly terrain will be difficult without knowledge of both $\bar{u}\partial\bar{c}/\partial x$ and $\bar{w}\partial\bar{c}/\partial z$. Furthermore, by accounting for only one of these two terms, for example by including $\bar{w}\partial\bar{c}/\partial z$ in the mass balance calculation, a term that can be measured at a single tower (Lee, 1998), a large (and systematic) bias in inferred canopy sources and sinks is likely to occur. This error may be larger than ignoring both advection terms.

In summary, this model study has indicated the dominant role of advection in the scalar mass balance for CO₂ transport on a forested hill. While the direct effects of topographic forcing on photosynthesis are small, the errors involved in ignoring one or both advection terms when inferring net ecosystem productivity from flux measurements on a single tower are sufficient to invalidate the estimates of net canopy exchange using eddy covariance measurements. It should be emphasized that the example of a two-dimensional hill maximizes the flow perturbation and, therefore these errors, but even in gentle three-dimensional terrain, errors of order 100% can be anticipated if advection is ignored. Furthermore, these model calculations were conducted, (i) for idealized conditions, including steady state and neutral flows, constant air temperature and vapour pressure deficit within the canopy, and constant forest floor respiration, and (ii) using an analytical model for \bar{u} and \bar{w} accompanied with several simplifications (see FB04). Caution must be exercised in any extrapolation of these model results to specific field conditions.

Acknowledgements

The first author acknowledges support from the Nicholas School of the Environment and Earth Sciences and the Center on Global Change (Duke University), and the Commonwealth Science and Industrial Research Organization (CSIRO) during a sabbatical leave at the FC Pye laboratory in Canberra, Australia in 2002. Additional support was provided by the National Science Foundation (NSF-EAR-0208258), the Office of Science (BER), U.S. Department of Energy–Cooperative Agreement No. DE-FC02-03ER63613 and the Terrestrial Carbon Processes Program (TCP). R. Leuning acknowledges support by the Australian Greenhouse Office through the CSIRO Climate Science Program.

Appendix A: Numerical Solution to the Scalar Transfer

With a first-order closure model approximation to $\overline{w'c'}$, the scalar mass balance can be expressed as a second-order ordinary differential equation, given by

$$-K_c \frac{\partial^2 \bar{c}}{\partial z^2} + \left(\bar{w} - \frac{\partial K_c}{\partial z} \right) \frac{\partial \bar{c}}{\partial z} + a(z) g_{\text{eff}} \bar{c} = a(z) g_{\text{eff}} \bar{C}_i - \left(\bar{u} \frac{\partial \bar{c}}{\partial x} \right) - \frac{\partial F_{\text{cx}}}{\partial x} \quad (\text{A1})$$

subject to the following boundary conditions:

$$\begin{cases} z = l_i; \bar{c} = C_o \\ z = -h_c; -K_c \frac{\partial \bar{c}}{\partial z} = R_E(x) \text{ or } \bar{c} = C_{\text{surface}} \end{cases} \quad (\text{A2})$$

The solution is generated iteratively as follows:

1. Use central difference to approximate all first-order and second-order concentration derivatives. Hence, Equation (A1) can be written as an algebraic second-order difference equation, of the form:

$$\begin{aligned} & \left[\frac{b_1(j)}{\Delta z^2} + \frac{b_2(j)}{2\Delta z} \right] \bar{c}(j+1) + \left[b_3(j) - \frac{2 \times b_1(j)}{\Delta z^2} \right] \bar{c}(j) \\ & + \left[\frac{b_1(j)}{\Delta z^2} - \frac{b_2(j)}{2\Delta z} \right] \bar{c}(j-1) = b_4(j), \end{aligned}$$

where

$$\begin{aligned} b_1 &= -K_c, \\ b_2 &= \bar{w} - \frac{\Delta K_c}{\Delta z}, \\ b_3 &= a g_{\text{eff}}, \\ b_4 &= a g_{\text{eff}} \bar{C}_i - \bar{u} \frac{\Delta \bar{c}}{\Delta x} - \frac{\Delta F_{\text{cx}}}{\Delta x}, \end{aligned}$$

and j is a height index ($j=1$ is the forest floor, and $j=N_z=(l_i+h_c)/\Delta z$ is the upper domain height).

2. Generate $Q_p(x, z)$ using the radiative transfer scheme described in Equations (15) to (17).
3. Assume $\bar{c} = C_o$ and solve for g_{eff} and \bar{C}_i using Equations (9)–(13).
4. With initial guesses on g_{eff} and \bar{C}_i , and initially assuming $\frac{\partial \bar{c}}{\partial x} = 0$, solve Equation (A1) using the tridiagonal solver (tridag) (Press et al., 1992).
5. Repeat steps 3–4 but use the solution from step (4) instead of $\bar{c} = C_o$.
6. Convergence is achieved when the maximum difference between two successive iterations is 1%.

References

- Albertson, J. D., Katul, G. G., and Wiberg, P.: 2001, 'Relative Importance of Local and Regional Controls on Coupled Water, Carbon, and Energy Fluxes', *Adv. Water Res.* **24** (9–10), 1103–1118.
- Baldocchi, D., Falge, E., Gu, L. H., Olson, R., Hollinger, D., Running, S., Anthoni, P., Berhofer, C., Davis, K., Evens, R., Fuentes, J., Goldstein, A., Katul, G., Law, B., Lee, X. H., Malhi, Y., Meyers, T., Munger, W., Oechel, W., Paw, K. T., Polegaard, U. K., Schmid, H. P., Valentini, R., Verma, S., Vesala, T., Wilson, K., Wofsy, S.: 2001, 'FLUXNET: A New Tool to Study the Temporal and Spatial Variability of Ecosystem – Scale Carbon Dioxide, Water Vapor, and Energy Flux Densities', *Bull. Amer. Meteorol. Soc.* **82**, 2415–2434.
- Belcher, S. E., and Hunt, C. R.: 1998, 'Turbulent Flow over Hills and Waves', *Ann. Rev. Fluid Mech.* **30**, 507–538.
- Belcher, S. E., Jerram, N., and Hunt, J. C. R.: 2003, 'Adjustment of a Turbulent Boundary Layer to a Canopy of Roughness Elements', *J. Fluid Mech.* **488**, 369–398.
- Brunet, Y., Finnigan, J. J., and Raupach, M. R.: 1994, 'A Wind-Tunnel Study of Air-flow in Waving Wheat—Single-Point Velocity Statistics', *Boundary-Layer Meteorol.* **70**, 95–132.
- Campbell, G. S. and Norman, J. M.: 1998, *An Introduction to Environmental Biophysics*, Springer, New York, 286 pp.
- Collatz, G. J., Ball, J. T., Grivet, C., and Berry, J. A.: 1991, 'Physiological and Environmental Regulation of Stomatal Conductance, Photosynthesis and Transpiration: A Model that Includes a Laminar Boundary Layer', *Agric. For. Meteorol.* **54**, 107–136.
- Carruthers, D. J. and Hunt, J. C. R.: 1990, 'Fluid Mechanics of Airflow over Hills: Turbulence, Fluxes, and Waves in the Boundary Layer', in *Atmospheric Processes over Complex Terrain, Meteorological Monographs*, Vol. 23, American Meteorological Society, Boston; MA, pp. 83–103.
- Denmead, O. T. and Bradley, E. F.: 1985, 'Flux Gradient Relationships in a Forest Canopy', in B. A., Hutchison and B. B. Hicks (eds), *The Forest-Atmosphere Interaction*, D. Reidel Publishing, Norwell, Mass., 421–422.
- Farquhar, G. D., Von Caemmerer, S., and Berry, J. A.: 1980, 'A Biochemical Model of Photosynthetic CO₂ Assimilation in Leaves of C₃ Species', *Planta* **149**, 78–90.
- Feigenwinter, C., Bernhofer, C., and Vogt, R.: 2004, 'The Influence of Advection on the Short Term CO₂ Budget in and Above a Forest Canopy', *Boundary-Layer Meteorol.*, in press.
- Finnigan, J. J.: 1985, 'Turbulent Transport in Plant Canopies' in B. A. Hutchinson and B. B. Hicks (eds), *The Forest-Atmosphere Interactions*, D. Reidel Publishing, Norwell, Mass., pp 443–480.
- Finnigan, J. J.: 1998, 'Air Flow over Complex Terrain', in W. L. Steffen and O. T. Denmead (eds), *Flow and Transport in the Natural Environment, Advances and Applications*, Springer, Berlin, pp 183–229.
- Finnigan, J. J.: 2000, 'Turbulence Inside Plant Canopies', *Ann. Rev. Fluid Mech.* **32**, 519–571.
- Finnigan, J. J.: 2004, 'Advection and Modeling', in X. Lee and W. J. (eds), *Handbook of Micrometeorology: A Guide for Surface Flux Measurements*, Kluwer Academic Publishers, Dordrecht, 209–244.
- Finnigan, J. J. and Raupach, M. R.: 1987, 'Transfer Process Within Plant Canopies in Relation to Stomatal Characteristics', in E. M. Zeiger, G. D. Farquhar and I. R. Cowan (eds), *Stomatal Function*, Stanford University Press, Stanford, CA, 385 pp.
- Finnigan, J. J. and Belcher, S. E.: 2004, 'Flow over Hill Covered with a Plant Canopy', *Quart. J. Roy. Meteorol. Soc.* **130** (596), 1–29 Part A.

- Hunt, J. C. R., Leibovich, S., and Richards, K. J.: 1998, 'Turbulent Shear Flows over Low Hills', *Quart. J. Roy. Meteorol. Soc.* **114**, 1435–1470.
- Jackson, P. S. and Hunt, J. C. R.: 1975, 'Turbulent Wind Flow over a Low Hill', *Quart. J. Roy. Meteorol. Soc.* **101**, 929–955.
- Kaimal, J. C. and Finnigan J. J.: 1994, *Atmospheric Boundary Layer Flows: Their Structure and Measurement*, Oxford University Press, New York, 289 pp.
- Katul, G. G., Mahrt, L., Poggi, D., and Sanz, C.: 2004, 'One and Two Equation Models for Canopy Turbulence', *Boundary-Layer Meteorol.* **113**, 81–109.
- Katul, G. G., Ellsworth, D., and Lai, C. T.: 2000, 'Modeling Assimilation and Intercellular CO₂ from Measured Conductance: A Synthesis of Approaches', *Plant, Cell Environ* **23**, 1313–1328.
- Katul, G. G. and Chang, W. H.: 1999, 'Principal Length Scales in Second-order Closure Models for Canopy Turbulence', *J. Appl. Meteorol.* **38**, 1631–1643.
- Katul, G. G., Geron, C. D., Hsieh, C. I., Vidakovic, B., and Guenther, A. B.: 1998, 'Active Turbulence and Scalar Transport Near the Land-Atmosphere Interface', *J. Appl. Meteorol.* **37**, 1533–1546.
- Lai, C. T., Katul, G. G., Butnor, J., Ellsworth, D., and Oren, R.: 2002, Modelling Night-time Ecosystem Respiration by a Constrained Source Optimization Method, *Global Change Biol* **8**, 124–141.
- Lai, C. T., Katul, G. G., Oren, R., Ellsworth, D., and Schäfer, K.: 2000, 'Modeling CO₂ and Water Vapor Turbulent Flux Distributions Within a Forest Canopy', *J. Geophys. Res.* **105**, 26333–26351.
- Lee, X.: 1998, 'On Micrometeorological Observations of Surface-air Exchanges over Tall Vegetation'. *Agric. Forest Meteorol.* **91**, 39–49.
- Leuning, R.: 1995, 'A Critical Appraisal of a Combined Stomatal-Photosynthesis Model for C₃ Plants', *Plant, Cell Environ* **18**, 339–355.
- Massman, W. J., and Weil, J. C.: 1999, 'An Analytical One-dimensional Second Order Closure Model of Turbulence Statistics and the Lagrangian Time Scale Within and Above Plant Canopies of Arbitrary Structure', *Boundary-Layer Meteorol.* **91**, 81–107.
- Physick W. L. and Garratt, J. R.: 1995, 'Incorporation of a High Roughness Lower Boundary Into a Mesoscale Model for Studies of Dry Deposition over Complex Terrain', *Boundary-Layer Meteorol.* **74**(1–2), 55–71.
- Pinard, J. P. and Wilson, J. D.: 2001, 'First- and Second Order Closure Models for Wind in a Plant Canopy', *J. Appl. Meteorol.* **40**, 1762–1768.
- Poggi, D., Porporato, A., Ridolfi, L., Albertson, J. D., and Katul, G. G.: 2004a, 'The Effect of Vegetation Density on Canopy Sub-Layer Turbulence', *Boundary-Layer Meteorol.* **111**, 565–587.
- Poggi, D., Katul, G. G., and Albertson, J. D.: 2004b, 'A Note on the Contribution of Dispersive Fluxes to Momentum Transfer within Canopies', *Boundary-Layer Meteorol.* **111**, 615–621.
- Press, W. H., Teukolsky, S. A., Vetterling, W., Flannery, B. P.: 1992, *Numerical Recipes in Fortran: The Art of Scientific Computing* 2nd edn, Cambridge University Press, New York, 963 pp.
- Raupach, M. R. and Finnigan, J. J.: 1997, 'The Influence of Topography on Meteorological Variables and Surface-Atmosphere Interactions', *J. Hydrol.* **190**, 182–213.
- Raupach, M. R., Finnigan, J. J., and Brunet, Y.: 1996, 'Coherent Eddies and Turbulence in Vegetation Canopies: The Mixing Layer Analogy', *Boundary-Layer Meteorol.* **78**, 351–382.
- Raupach, M. R., Weng, W. S., Carruthers, D. J., and Hunt, J. C. R.: 1992, 'Temperature and Humidity Fields and Fluxes over Low Hills', *Quart. J. Roy. Meteorol. Soc.* **118**, 191–225.

- Taylor, P. A., Mason, P. J., and Bradley, E. F.: 1987, 'Boundary Layer Flow over Low Hills', *Boundary-Layer Meteorol.* **39**, 15–39.
- Wilson, J. D., Finnigan, J. J., and Raupach, M. R.: 1998, 'A First Order Closure for Disturbed Plant-canopy Flows and Its Application to Winds in a Canopy on a Ridge', *Quart. J. Roy. Meteorol. Soc.* **124**, 705–732.
- Wilson, N. R. and Shaw, R. H.: 1977, 'A Higher Order Closure Model for Canopy Flow', *J. Appl. Meteorol.* **16**, 1198–1205.